EUROPEAN ORGANIZATION FOR NUCLEAR RESEARCH

Proposal to the ISOLDE and Neutron Time-of-Flight Committee

Neutron emission from unbound states in ^{135}Sn

28/09/2021

R. Grzywacz[1,2], A. Korgul[3], M. Madurga[1], L. M. Fraile[4], Z. Xu[1], M. Piersa-Siłkowska[3], J. Benito[4], A. Algora[5], J.M. Allmond[2], D. Bardayan[6], P. Bielak[3], A. Fijałkowska[3], L.P. Gaffney[7], V. Guadilla[3], J. Heideman[1], C. Henrich[8] S. Neupane[1],T. King[1], N. Kitamura[1], Ł. Koszuk[3], M. J. García Borge[9], A. Illana[10,11], Z. Janas[3], K.L. Jones[1], A. Kankainen[12], M. Karny[3], T. Kawano[13], K. Kolos[14], T. Kröll[8], A. Lama[12] R.Lică[14], M. Llanos[4], A.I. Morales[5] C. Mazzocchi[3], C. Mihai[15], K. Miernik[3], J.R. Murias[6], S.E.A. Orrigo[5] , R.D. Page[7], Zs. Podolyák[16], W. Poklepa[3], B.C. Rasco[2], M.M. Rajabali[17], B. Rubio[5] M. Rudigier[8], K. Rykaczewski[2], K. Siegl[1], M. Singh[1], M. Stepaniuk[3], M. Stryjczyk[12], K. Solak[3], C. Sotty[8], O. Tengblad[8], M. Tresckow[8], N. Warr[18], K. Wimmer[19], H. DeWitte[20], R. Yokoyama[1].

[1] Dept. of Physics and Astronomy, University of Tennessee, Knoxville, Tennessee 37996, USA.
[2] Physics Division, Oak Ridge National Laboratory, Oak Ridge, Tennessee 37830, USA.
[3] Faculty of Physics, University of Warsaw, PL 00-681 Warsaw, Poland.
[4] Grupo de Física Nuclear & IPARCOS, Universidad Complutense de Madrid, E-28040, Spain.
[5] Instituto de Física Corpuscular, Edificio de Institutos de Paterna, E-46071 Valencia, Spain.
[6] Institute for Structure and Nuclear Astrophysics, Department of Physics, Notre Dame, Indiana 46556, USA.
[7] The University of Liverpool, Liverpool L69 7ZE, United Kingdom.
[8] Technische Universität Darmstadt, Institut für Kernphysik, D-64289 Darmstadt, Germany
[9] Instituto de Estructura de la Materia, E-28006 Madrid, Spain.
[10] University of Jyväskylä, Department of Physics, Jyväskylä, Finland.
[11] Helsinki Institute of Physics, Helsinki, Finland.
[12] Department of Physics, University of Jyväskylä, Finland.
[13] Theoretical Division, Los Alamos National Laboratory, Los Alamos, NM 87545, USA .
[14] Lawrence Livermore National Laboratory, Livermore, California 94550, USA.
[15] National Institute of Physics and Nuclear Engineering, RO-077125 Bucharest, Romania.
[16] Department of Physics, University of Surrey, Guildford GU2 7XH, United Kingdom
[17] Tennessee Technological University, Cookeville, Tennessee, USA.
[18] Institut für Kernphysik, Universität zu Köln, Germany.
[19] Instituto de Estructura de la Materia, CSIC, E-28006 Madrid, Spain
[20] KU Leuven, Instituut voor Kern-en Stralingsfysica, 3001 Leuven, Belgium.

Spokesperson(s): Robert Grzywacz (University of Tennessee, ORNL), rgrzywac@utk.edu
Agnieszka Korgul (University of Warsaw), korgul@fuw.edu.pl
Miguel Madurga (University of Tennessee), Miguel.madurga@gmail.com
Luis Mario Fraile (Universidad Complutense de Madrid), lmfraile@ucm.es
Local contact: Razvan Lică, razvan.lica@cern.ch

CERN-INTC-2021-050 / INTC-P-614
28/09/2021

Abstract

We propose to study beta-delayed neutron emission from ^{135}In using Isolde Decay Station neutron and gamma detectors and the new high-resolution neutron detector NEXT. The experiment aims to perform high-statistics and high-resolution spectroscopy of neutrons, which are emitted from excited states in ^{135}Sn. The experiment addresses multiple goals relevant to nuclear structure and astrophysics and will focus on testing the predictive power

of nuclear models for ^{135}In decay, developed and constrained by recent results from ^{133}In and ^{134}In decay experiments. Due to large Q_β-$S_{1n,2n}$ values, one and two neutron-unbound states in ^{135}Sn will be populated. This will allow us to map the beta decay strength distribution through the use of neutron and gamma-ray spectroscopy. This experiment's main goal is to identify the excitation energy and degree of fragmentation of the main Gamow-Teller transition. We will also explore the relative role of the first-forbidden transitions, which are expected to provide a competing neutron emission channel sufficient to locate the $h_{11/2}$ hole state in ^{135}In. The neutron-gamma coincidences combined with the statistical model will enable us to study new states in ^{134}Sn and constrain their spin assignments.

Requested shifts: 16 shifts

Introduction: Beta-delayed neutron and gamma spectroscopy of ^{133}In and ^{134}In postulated the fundamental picture for the beta-decay southeast of ^{132}Sn [Pie19, Pie21, Xu21, Hei21]. Beta-decay in this region is driven predominantly by the single Gamow-Teller (GT) transition of a $g_{7/2}$ neutron into a $g_{9/2}$ proton, which generates a neutron-unbound resonance at 6-7 MeV excitation energy in the daughter. The First-Forbidden (FF) transitions connect opposite-parity proton and neutron orbitals, which are closer to the Fermi surface. Despite their smaller transition matrix elements, they are enhanced by the phase-space factor and provide a strong decay channel competing with the Gamow-Teller transition. Understanding the role of the GT and FF transitions is one of the key contributions of nuclear beta decay studies to the r-process modelling. The detailed measurements of the strength distribution provide key input to test nuclear models, which aim to predict nuclear lifetimes and decay branching ratios.

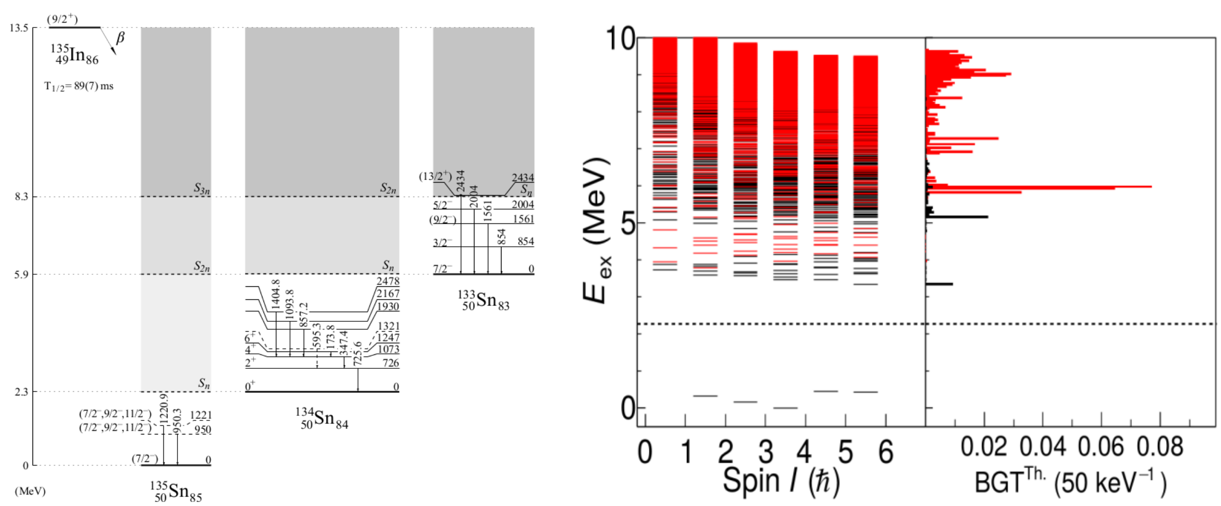

Figure 1. Beta decay of ^{135}In established by Piersa et al. [Pie21]. The neutron unbound states in ^{135}Sn will decay via neutron emission to neutron bound and unbound states in ^{134}Sn. (Right) Shell-model predictions for the excited states in ^{134}Sn and Gamow- Teller (red) and First Forbidden (black) strength distribution using LSSM with N3LO interactions [Xu21]. The calculations were done for the $J=9/2^+$ spin and parity of the ^{135}In ground state.

Most of the r-process nuclei are beta-delayed multi-neutron emitters and astrophysics models require reliable predictions of the beta-decay half-lives and neutron emission branching ratios. The measurements close to doubly-magic numbers are of particular importance because of the strong constraints imposed on the nuclear models and relative simplicity of the calculations. While the ^{133}In decay experiment [Xu21] provided a base picture for the beta-decay model, the ^{134}In neutron spectroscopy study [Hei21] focused on validating the statistical model description of the neutron emission from excited states in ^{134}Sn. We have found, using the Los Alamos BeoH code [Low21], that the statistical model could not describe the population of excited states in ^{133}Sn under the compound nucleus assumption. This was achieved by combining detailed measurement of neutron emission branching ratios from the Gamow-Teller resonance in ^{134}Sn to single-particle states in ^{133}Sn. The high-statistics exploration of this effect is the subject of the IDS-approved proposal [Grzy20] addressing the beta-n decay of ^{134}In, which will investigate the departure from statistical model predictions with higher accuracy and for expanded groups of states, including FF transitions, and explore the details of the 2n emission. The study of the ^{135}In decay provides a unique opportunity to investigate the details of two-neutron emission to single-particle excited states in ^{133}Sn, especially to the newly discovered $i_{13/2}$ state [Pie21]. Within the compound nucleus postulate [Kaw16] for a given decay strength distribution,

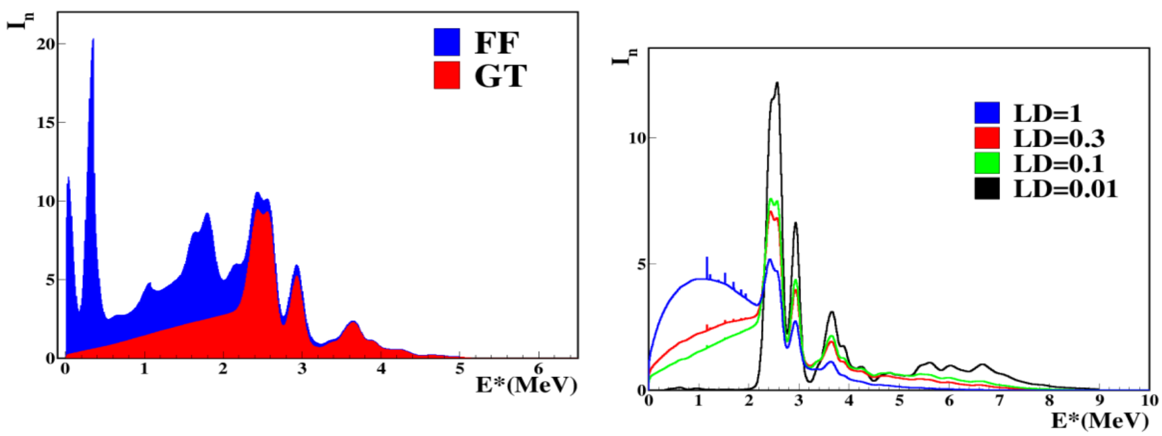

Figure 2. (Left) Expected neutron spectrum of ^{135}In using shell-model predictions (GT in red and FF in blue) combined with the statistical model predictions simulated using BeoH code [Kaw19]. (Right) The same neutron spectrum modeled with various level-density parameters showing the sensitivity of two-neutron emission to level densities in ^{134}Sn. The black spectrum shows almost no two-neutron emission and blue is calculated for nominal level densities. Here only the GT mode was considered. The red and green histograms are intermediate scenarios.

the 2n emission branching ratio and relative population of the states in ^{133}Sn depend mainly on the level density in the intermediate nucleus ^{134}Sn. Combining the neutron emission model with detailed neutron-gamma spectroscopy will constrain the spin assignments for the involved nuclei due to the sensitivity of neutron emission to the centrifugal barrier, see Figure 4.

The ground state beta-decay energy is high, about Q_β=13.5 MeV, and the daughter nucleus ^{135}Sn has low one- and two-neutron separation energies S_n=2.3 MeV and S_{2n}=5.9 MeV, respectively. The expected Gamow-Teller decay will be similar to ^{133}In ($\nu g_{7/2} \rightarrow \pi g_{9/2}$ E*~6 MeV) in energy but is predicted to be more fragmented due to the increased role of correlations in the N=86 ^{135}In nucleus. This fragmentation effect was already observed in ^{134}In decay [Hei21]. These excited GT states are also predicted to be slightly above the two-neutron separation energy in ^{135}Sn. The presence of two valence neutrons outside the N=82 closed-shell leads to a much higher density of excited states in ^{134}Sn, which may be reflected in the observed beta-decay properties. Thus, the ^{135}In neutron emission may be closer to the statistical model predictions.

The experiment will attempt a detailed study of neutron and gamma-ray spectroscopy using IDS neutron time-of-flight array and IDS clover detectors required to reconstruct the level scheme properly. In addition, we will complement this system with the NEXT neutron array [Hei19], which will provide a much better energy resolution for the neutron TOF measurement, achieved by localizing neutron interaction in a segmented array. This is especially important for high-energy neutrons. Moreover, its capability in neutron-gamma discrimination can reduce gamma background in the neutron spectrum.

Goals of experiments: The decay of βn precursor ^{135}In will address multiple goals, which all can be achieved in a single measurement with the IDS experimental setup.

<u>*The first goal*</u> for this experiment will be a measurement of the main Gamow-Teller decay channel $\nu g_{7/2} \rightarrow \pi g_{9/2}$ via its neutron emission. In the shell model prediction this transformation will populate a group of neutron-unbound states at about 6 MeV excitation energy, see Figure 1. The decay of this group of resonances proceeds via neutron-gamma cascades to the excited states in ^{134}Sn. Two-neutron emission is also possible if the excitation energy is higher than S_{2n}=5.9 MeV.

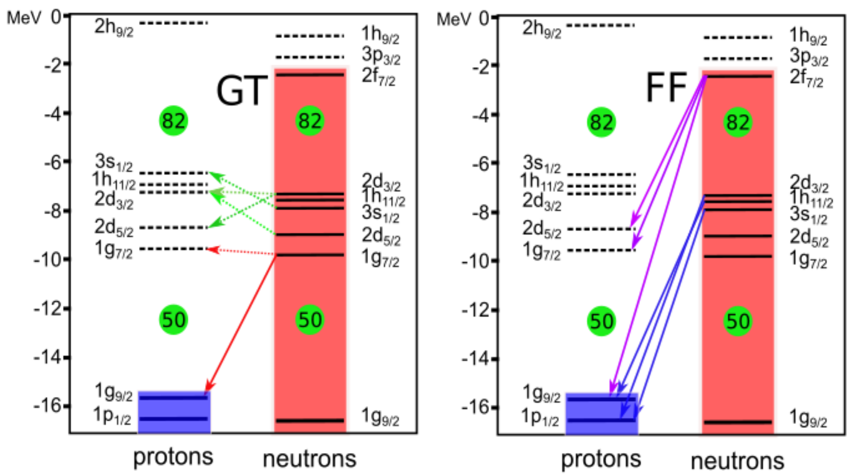

Figure 3. Single particle states near ^{132}Sn and schematic representation of the dominant decay channels for the Gamow-Teller and First Forbidden modes.

The fragmentation of the neutron spectrum will require efficient neutron-gamma coincidence measurement. Figure 1 shows the prediction of the strength distribution obtained with the shell-model calculation and N3LO residual interactions [Ent03, Xu21], which provided a good agreement between experiment and theory for ^{133}In and ^{134}In decays. To assess the degree of the decay fragmentation, we have performed the calculation for the neutron spectrum using the Los Alamos Hauser Feshbach (HF) BeoH code [Kaw16, Kaw19]. Here, neutron emission probabilities are only determined by the optical model parameters and not by details of the nuclear states' structure (wave functions). The measurement of the spectrum and thus the fragmentation of the strength thus is essential to establish systematics of the GT quenching near doubly magic nuclei. Furthermore, Gamow-Teller strength measurements are required to benchmark recently developed nuclear theories [Gys19] of the origin of the GT strength quenching. The ^{133}In measurement, which is the closest to doubly magic ^{132}Sn, was a base point establishing the position and strength of the main GT resonance. The measurement of ^{135}Sn will verify how robust the model prediction is when moving further away from stability

<u>*This experiment's second goal*</u> is to measure two-neutron emission probabilities from the excited states in ^{135}Sn. With the relatively low two-neutron separation energy (S_n=2.3 MeV) of ^{135}Sn the experiment offers a unique opportunity to study details of this process, such as energy correlations between neutrons, terra incognita for the decay of heavy nuclei. Here,

the single-particle states in ^{133}Sn are populated [Pie21], but neutron spectroscopy is required to establish from which excited states in ^{135}Sn they originate. This is essential for a complete determination of the beta-decay strength distribution. In addition to two-neutron emission, two-neutron unbound states are known to decay via emission of a single neutron [Yok19, Mol19].

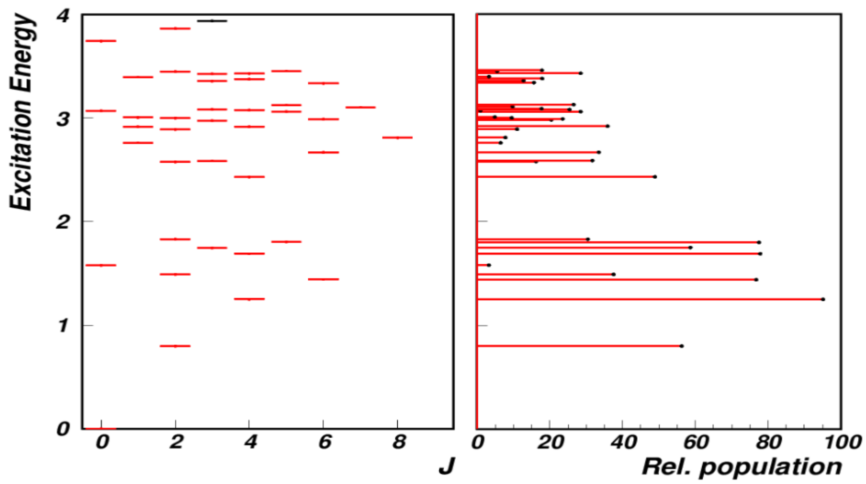

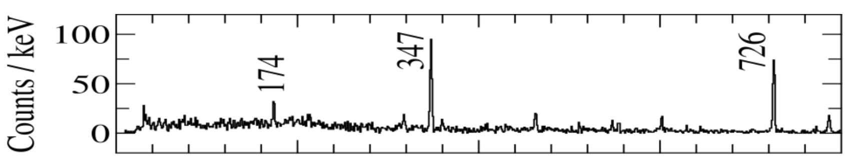

Figure 4 (Top) The spectrum of excited states in ^{134}Sn predicted by the shell model calculation (Left) and their relative population (Right) in the ^{135}In decay obtained with the BeoH statistical model with the B(GT) strength distribution from the shell model. (Bottom) Gamma-ray spectrum collected for ^{135}In [Pie21] showing the relative ratio of 726, 347 and 174 keV lines from the de-excitation of the lowest 2^+, 4^+ and 6^+ states in ^{134}Sn respectively.

Our investigation with the statistical model shows a strong sensitivity of two neutron emissions to the level densities in ^{134}Sn, see Figure 3. The highest P_{2n} and strong population of excited states in ^{133}Sn are predicted for the nominal Gilbert-Cameron level density parameters used by the BeoH code. By reducing the level density parameter by a factor of 100, the decay of ^{135}In proceeds exclusively via single neutron emission. It will also result in a very "hard" neutron energy spectrum with the emission of 2-8 MeV neutrons. The calculations were made using the shell-model strength distribution and BeoH statistical model, see Figure 2. The use of the NEXT detector is essential due to its high-resolution energy measurement capability.

The third goal of this proposal will be direct identification of the First-Forbidden transitions to neutron unbound states in ^{135}Sn. As can be inferred from the measurement of the ^{133}In decay [Xu21], FF transitions should play an important role in the decay of ^{135}In. There, the FF transition connected opposite parity states with strong single-particle components, see Figure 3. In the case of ^{133}In, these states deexcite primarily via neutron emission but also, surprisingly, via gamma-ray emission. The shell-model predictions in Figure 1 show the expected distribution of the FF-strength distribution with strong contributions at 3 and 5 MeV excitation energy, the first of which was attributed to the dominant $(\nu h_{11/2})^{-1}$ component. Understanding the relative importance of GT and forbidden transitions in the neutron-rich nuclei is needed to constrain global model predictions for the r-process nuclei [Mol03].

The fourth goal of this proposal will focus on the expansion of the ^{134}Sn and ^{135}Sn level schemes. The statistical model predicts all of the bound states in ^{134}Sn up to 6^+ states to be populated. In this case, due to the role of a centrifugal barrier the decays to 4^+ and 6^+ states will be favored. The 2^+ states will be less favorable but still strongly populated as evidenced by experimental results [Pie21]. Identifying the unknown first excited 0^+ in ^{134}Sn (at about E*=1.5 MeV, see Fig. 4) will be especially attractive. This state is predicted to be weakly populated in the neutron emission from ^{135}Sn, but with sufficient statistics, it can be identified and assigned based on neutron-gamma coincidences and relative population intensities.

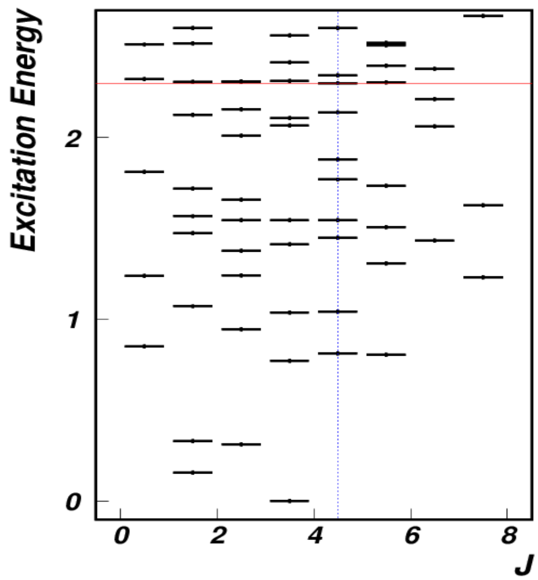

Figure 5. The spectrum of negative parity bound excited states in ^{135}Sn predicted by the shell model calculation with jj56pn residual interactions. A vertical line is drawn for J=9/2 to indicate the likely states which may be populated in the FF transitions.

The previous study of the ^{135}In decay has shown that the bound states in ^{135}Sn are populated very weakly. Nevertheless a longer high statistics experiment should improve this situation. Figure 5 shows the results of the shell-model predictions with jj56pn interactions for the low-lying excited states in ^{135}Sn. We will also search for evidence of gamma-decay of neutron unbound states in the ^{135}Sn, similar to the ~6 MeV transitions observed in ^{133}In decay [Pie18,Xu21,Vaq17]. They are crucial to understand the role of nuclear structure in beta delayed neutron emission which may result in unusual hindrance for certain decays.

Experimental setup: The experiment will be instrumented at the ISOLDE Decay Station using its standard set of 4 clover detectors, ~4% efficiency at 1 MeV, the IDS in-vacuum beta detector, 90% electron detection efficiency, and the newly commissioned IDS Neutron DEtector (INDiE) using VANDLE array detector design and electronics [Pau14,Pet16]. The angular acceptance for 26 scintillator bars at 100 cm is Ω=11% of 4π, and using 90% beta efficiency, the total efficiency of the array is between 3-5%. The performance of this system was demonstrated during the ^{133}In decay experiment. The neutron detection will be enhanced by 30 NEXT neutron detector modules, which will have much higher neutron energy resolution due to their segmentation and provide an additional 6% neutron detection efficiency. These detectors are capable of neutron-gamma discrimination above 400 keV neutron energy, which is an added benefit for this measurement. These detectors will be operated at 50 cm TOF and will be placed on both sides of INDiE. Both detectors have a neutron detection threshold of about 100 keV.

Summary of requested shifts:

Table 1: Expected neutron rates. These calculations are done for 2 uC PS Booster beam (n.c. = neutron converter)

	P_{1n} (%)	Yield (ion/µC)	IDSND Eff	Neutrons (1/h)	Shifts	Target	Source
^{135}In	90%	4	0.04	700	15	UC_X+n.c.	Hot Ta line and cavity + RILIS
^{49}K	86%	>1000	0.04	>1.0 10^5	1	UCx	Hot Ta line and cavity

Table 1 summarizes the requested beam time. Due to the lack of evidence of a beta-decaying isomer in ^{135}In isotopes, we request the hot Ta ion source along with the RILIS ion source in broadband mode. Enhancement of In release using RILIS has been observed in several experiments at ISOLDE [Dil02], with yields of about 4 ions/uC for ^{135}In observed by Piersa et al. [Pie21]. The main isobaric components, and therefore contamination, in mass A=135 are the relatively long-lived isotopes of iodine and cesium. We will partially eliminate them by setting a high-threshold on the beta trigger detector. We request 15 shifts to collect about 3.5×10^6 decays of ^{135}In. This will enable detection of about 10^5 neutrons from the decay of ^{135}In, see [Grz20]. The calculations were made based on short measurements of ^{135}In. P_{1n}=0.9 and P_{2n}=0.1 were used, in accordance with the experimental values [Pie21]. High neutron statistics is required for the mapping of the strength distribution and require neutron-gamma coincidence measurement. The number of ^{135}In decays will provide sufficient number of neutron-gamma coincidences to enable detection of about 50 counts in the decay cascade of excited 0^+ state populated with 1% branching ratio. During the 15 shifts we expect to collect about 300 "clean" two-neutron events. This number carries about 50% uncertainty due to the unknown spectrum of the neutrons observed in this process. The beam time breaks down into 15 shifts for ^{134}In and 1 shift for ^{49}K calibration.

References:

[Ent03] D.R. Entem & R. Machleidt, Phys. Rev. C **68**, 041001 (2003).

[Grz20] R. Grzywacz, M. Karny, M. Madurga et al. https://cds.cern.ch/record/2717898/files/INTC-P-554.pdf

[Gys19] P. Gysbers et al. Nature Physics **15**, 425–426 (2019).

[Hei19] J. Heideman, Nuclear Instruments and Methods A, **946** (2019) 162528.

[Hei21] J. Heideman et al. to be submitted

[Kaw08] T. Kawano, P. Moller, and W. B. Wilson, Phys. Rev. C **78**, 054601 (2008).

[Kaw19] T. Kawano, https://arxiv.org/abs/1901.05641.

[Kaw16] T. Kawano, R. Capote, S. Hilaire, and P. Chau Huu-Tai, Phys. Rev. C **94**, 014612 (2016).

[Lov21] A.E. Lovell ,T. Kawano, S. Okumura, I. Stetcu, M.R. Mumpower, and P. Talou Phys. Rev. C **103**, 014615 (2021)

[Mol19] Möller et al., Atomic Data and Nuclear Data Tables **125**, 1-192 (2019).

[Mum16] M.R. Mumpower, T. Kawano, and P. Möller, Phys. Rev. C **94**, 064317 (2016).

[Pau14] S. Paulauskas et al., Nuclear Instruments and Methods A **737**, 22 (2014).

[Pet16] W. Peters et al. Nuclear Instruments and Methods A **836**, 122 (2016).

[Pie18] M. Piersa et al. Phys. Rev. C **99**, 024304 (2019).

[Pie21] M. Piersa et al. Phys. Rev. C (2021) to be published.

[Vaq17] V. Vaquero, et al., Phys. Rev. Lett. **118**, 202502 (2017).

[Yok19] R. Yokoyama et al., Phys. Rev C **100**, 031302(R) (2019).

[Xu21] Z.Y. Xu et al. to be submitted (2021).

Appendix

DESCRIPTION OF THE PROPOSED EXPERIMENT

The experimental setup comprises: *(name the fixed-ISOLDE installations, as well as flexible elements of the experiment)*

Part of the Choose an item.	Availability	Design and manufacturing
[if relevant, name fixed ISOLDE installation: COLLAPS, CRIS, ISOLTRAP, MINIBALL + only CD, MINIBALL + T-REX, NICOLE, SSP-GLM chamber, SSP-GHM chamber, or WITCH]	☒ Existing	☒ To be used without any modification
	IDS	To be used as currently existing
[Part 1 of experiment/ equipment]	☐ Existing	☐ To be used without any modification ☐ To be modified
	☐ New	☐ Standard equipment supplied by a manufacturer ☐ CERN/collaboration responsible for the design and/or manufacturing
[Part 2 experiment/ equipment]	☐ Existing	☐ To be used without any modification ☐ To be modified
	☐ New	☐ Standard equipment supplied by a manufacturer ☐ CERN/collaboration responsible for the design and/or manufacturing
[insert lines if needed]		

HAZARDS GENERATED BY THE EXPERIMENT

(if using fixed installation) Hazards named in the document relevant for the fixed [COLLAPS, CRIS, ISOLTRAP, MINIBALL + only CD, MINIBALL + T-REX, NICOLE, SSP-GLM chamber, SSP-GHM chamber, or WITCH] installation.

Additional hazards:

Hazards	*[Part 1 of the experiment/equipment]*	*[Part 2 of the experiment/equipment]*	*[Part 3 of the experiment/equipment]*
Thermodynamic and fluidic			
Pressure	[pressure][Bar], [volume][l]		
Vacuum			
Temperature	[temperature] [K]		
Heat transfer			
Thermal properties of materials			
Cryogenic fluid	[fluid], [pressure][Bar], [volume][l]		
Electrical and electromagnetic			
Electricity	[voltage] [V], [current][A]		
Static electricity			
Magnetic field	[magnetic field] [T]		

Batteries	☐		
Capacitors	☐		
Ionizing radiation			
Target material	[material]		
Beam particle type (e, p, ions, etc)			
Beam intensity			
Beam energy			
Cooling liquids	[liquid]		
Gases	[gas]		
Calibration sources:	☐		
• Open source	☐		
• Sealed source	☐ [ISO standard]		
• Isotope			
• Activity			
Use of activated material:			
• Description	☐		
• Dose rate on contact and in 10 cm distance	[dose][mSV]		
• Isotope			
• Activity			
Non-ionizing radiation			
Laser			
UV light			
Microwaves (300MHz-30 GHz)			
Radiofrequency (1-300MHz)			
Chemical			
Toxic	[chemical agent], [quantity]		
Harmful	[chemical agent], [quantity]		
CMR (carcinogens, mutagens and substances toxic to reproduction)	[chemical agent], [quantity]		
Corrosive	[chemical agent], [quantity]		
Irritant	[chemical agent], [quantity]		
Flammable	[chemical agent], [quantity]		
Oxidizing	[chemical agent], [quantity]		
Explosiveness	[chemical agent], [quantity]		
Asphyxiant	[chemical agent], [quantity]		
Dangerous for the environment	[chemical agent], [quantity]		
Mechanical			
Physical impact or mechanical energy (moving parts)	[location]		
Mechanical properties (Sharp, rough, slippery)	[location]		
Vibration	[location]		
Vehicles and Means of Transport	[location]		
Noise			
Frequency	[frequency],[Hz]		
Intensity			
Physical			
Confined spaces	[location]		
High workplaces	[location]		

Access to high workplaces	[location]		
Obstructions in passageways	[location]		
Manual handling	[location]		
Poor ergonomics	[location]		

00.1 Hazard identification

3.2 Average electrical power requirements (excluding fixed ISOLDE-installation mentioned above): *(make a rough estimate of the total power consumption of the additional equipment used in the experiment)*

The INDiE detectors run at 1000 V and use 1 mA current on average, drawing 1 W each. The next detector have exactly the same power requirements. We will run 40 detectors, requiring 40 W.